Core @ double shell structured PBO composite with excellent dielectric properties and high heat resistance

Qiang Liu,[a] Zhipeng Cheng ,[a] Jun Qian,*[a] Xuexue Chen,[a] Yitong Zhang,[a] Haojie Li[a] and Qixin Zhuang*[a]

[a] *The Key Laboratory of Advanced Polymer Materials of Shanghai and Key Laboratory of Specially Functional Polymeric Materials and Related Technology, Ministry of Education, School of Materials Science and Engineering, East China University of Science and Technology, Shanghai 200237, China*

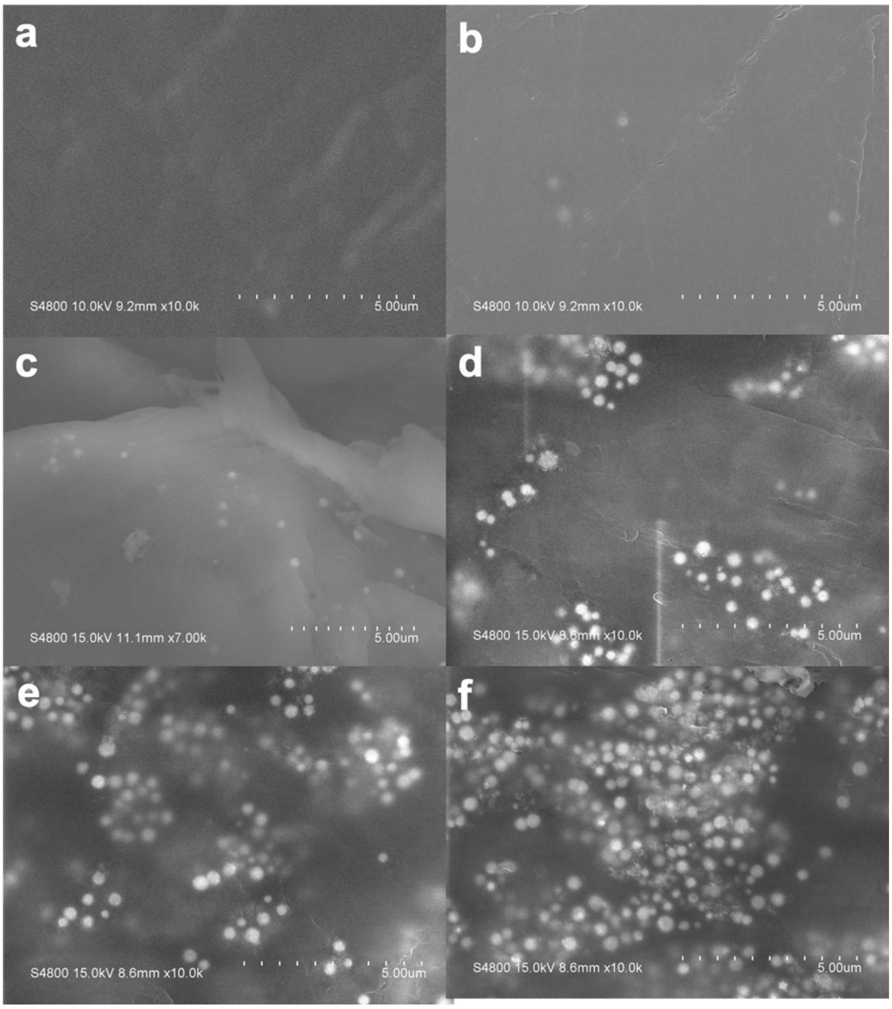

Fig. S1 SEM images of 0wt%, 3wt%, 6wt%, 9wt%, 12wt%, and 15wt%-Fe_3O_4@C@PANI /PBO

The distribution of the filler throughout the material is very uniform. when the mass fraction at 3wt%, 6wt% and 9wt%, We found almost every filler particle is dispersed; Almost all the fillers in Fig. 3e (at 1wt%) are also dispersed (Refer to the enlarged figure 5d in the original text); But, When the mass fraction reaches 15%, part of the fillers began to aggregate (in Fig. s1f).

The distribution of Fe_3O_4@C is similar to the Fe_3O_4@C@PANI. The distribution of the Fe_3O_4@C is uniform, but there are also subtle differences in concentration in the smaller area. Compare with Fe_3O_4@C@PANI, the difference is bigger. This phenomenon is obvious in the instrument screen.

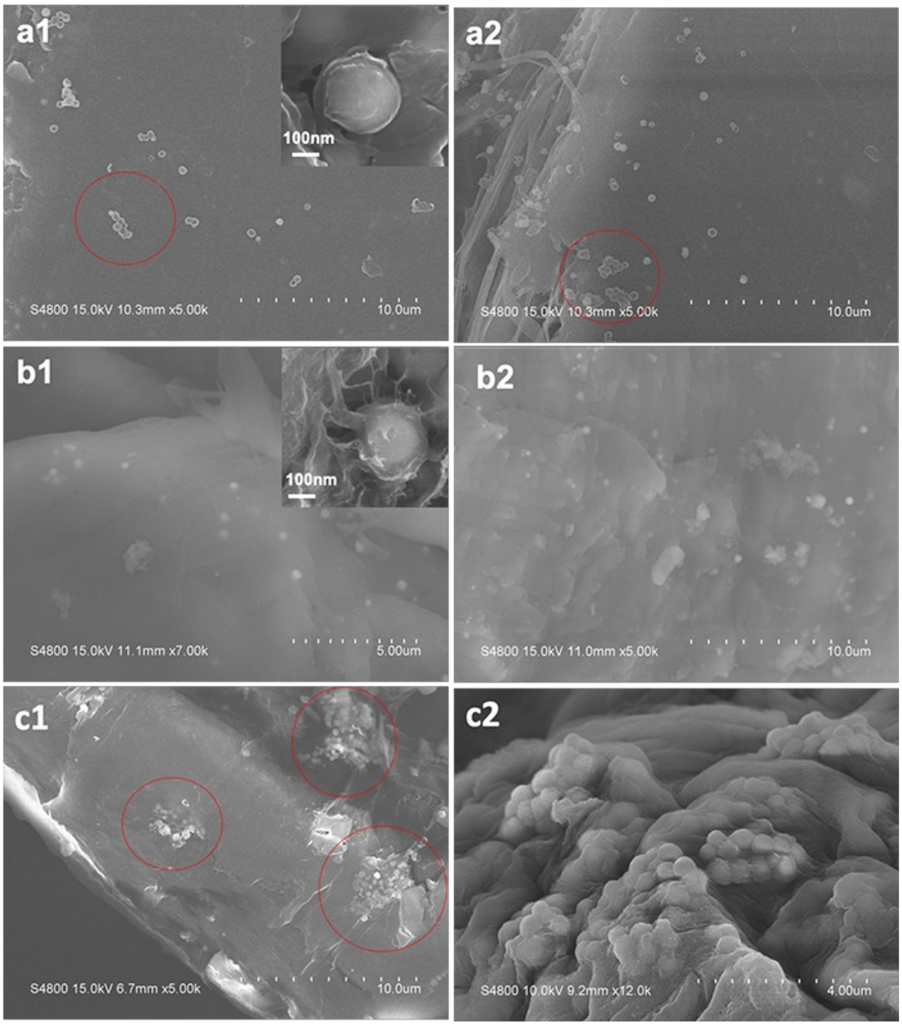

Fig. s2 SEM images of 6wt%-Fe_3O_4@C /PBO(a1/a2), 6wt%-Fe_3O_4@C@PANI /PBO(b1/ b2); Mix-6wt%-Fe_3O_4@C@PANI /PBO(c1/c2)

Table s1 dispersion of the filler in the matrix

film	Preparation	Distribution throughout the material	Distribution in small area	Figure
6wt%-Fe_3O_4@C /PBO	In-Situ Polymerization	good	medium	a1/a2
6wt%-Fe_3O_4@C@PANI /PBO	In-Situ Polymerization	good	good	b1/b2
Mix-6wt%-Fe_3O_4@C@PANI /PBO	Physical mixing	bad	bad	c1/c2

(a1/a2) and (b1/b2) are prepared by in-situ polymerization, but (c1/c2) is prepared by physical mixing method. First, from the perspective of the entire material area, the filler distribution of (a1/a2) and (b1/b2) are uniform, but the distribution of (c1/c2) is not uniform. We found that the fillers of (c1/c2) were all piled up in several areas, while the other areas had almost no filler. (as shown in Fig. c1, c2) Second, from the perspective of small area, the uniformity of (b1/b2) is better than (a1/a2)'s. As shown in (a1/a2), We can often observe a small group of Fe_3O_4@C nanoparticles in a small group, But this phenomenon is rarely seen in (b1/b2), and Almost all Fe_3O_4@C@PANI in (b1/b2) are individually separated.

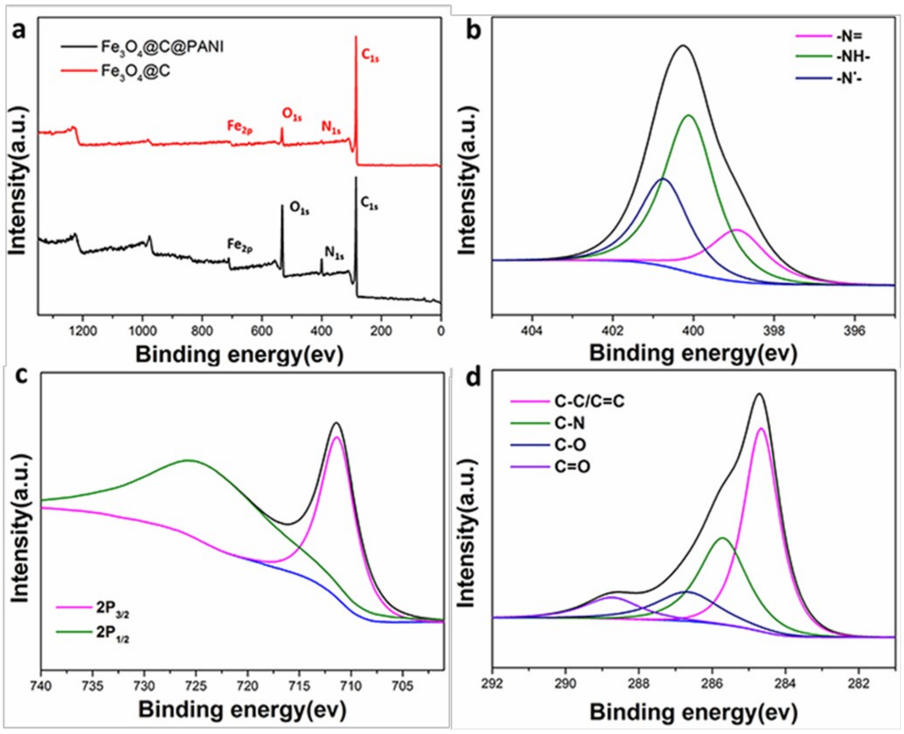

Fig. s3 XPS spectrum of (a) Fe_3O_4@C@PANI and Fe_3O_4@C; (b)/c)/ (d) XPS data of the N_{1s}, Fe_{2p} and C_{1s} regions of the Fe_3O_4@C@PANI, respectively

Compared with Fe_3O_4@C, Fe_3O_4@C@PANI has a distinct N_{1s} peak around 400, Which indicate that the N element is mainly from PANI. Fig. 8b is the spectrum of the N_{1s} of Fe_3O_4@C@PANI, which shows three different peaks at 398.9, 399.9 and 400.3 eV, corresponding to the–N=, –NH–, and–N^+- bonds, respectively.[1],[2, 3] The region of the C 1s spectrum can be decomposed into four components corresponding to C-C/C=C (284.6 eV), C-N (285.7 eV) , C-O (286.6 eV) and C=O(288.7 eV), respectively.[1] C-N bonds come from PANI molecular chain. The appearance of C-O (286.6 eV) and C=O (288.7 eV) are due to the subsequent acidification and polymerization process. Two broad peaks centered at 723.9 eV and 711.2 eV are assigned to the spin-orbit split doublet of Fe $_{2p1/2}$ and Fe $_{2p3/2}$, in accordance with the reported values for Fe_3O_4.[4] “The broadness of Fe $_{2p}$ peaks indicates the presence of dual iron oxidation states (Fe^{2+} and Fe^{3+})”[5, 6]

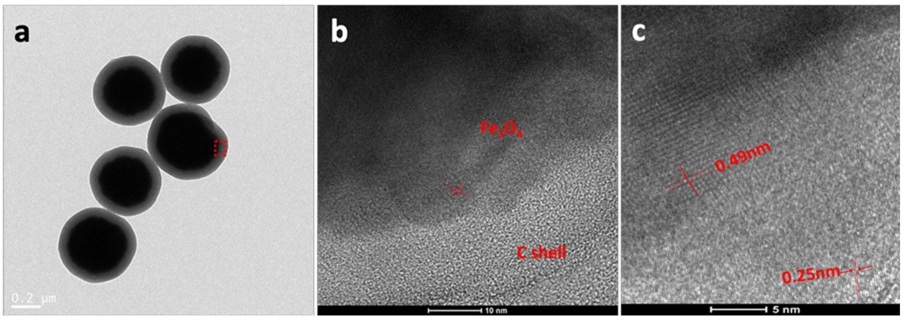

Fig.s4 (a-b) HRTEM of Fe_3O_4@C;(c) HRTEM of Fe_3O_4 (the the core part of Fe_3O_4@C)

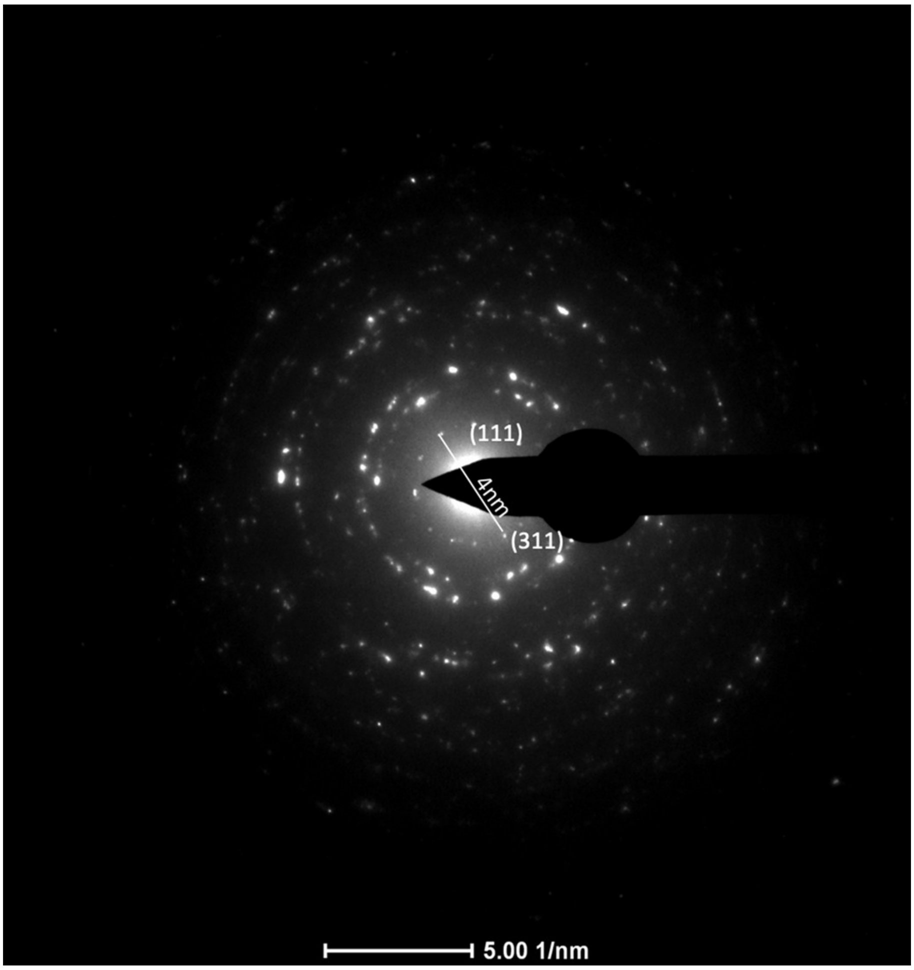

Fig. s5 SAED of Fe_3O_4

As is shown in fig. s4, HRTEM may tell the lattice information. I choose the interface of Fe_3O_4 and carbon as the observation area. We can see the boundaries of Fe_3O_4 and carbon in Fig. s4b. Fe_3O_4 is inverse spinel structure, so it has obvious lattice fringes. But carbon is amorphous carbon and don’t have clear lattice fringes. Fig. s4c shows that there are two kinds of lattice fringes of Fe_3O_4, and the corresponding interplanar spacing is 0.49nm (111) and 0.25 nm(311), respectively.

The selected area electron diffraction (SAED) pattern in Fig. s5 is composed of a series of concentric circles of different radii, which are produced by a large number of small grains of Fe_3O_4 in the irradiation zone.[6,7,5] . The diffracted beam produced by the same crystal face family forms a conical surface with a half-appoint angle of 2θ, and its line with the ground is a circle, and the radius of the ring is $R=L\lambda/d=K/d$， K and L is the instrument parameter. we can speculate that the aperture (radius 2 nm) near the bright spot corresponds to the (111) crystal plane. The aperture (radius 4n m) corresponds to the (311) crystal plane. The other apertures correspond to the other crystal planes in Fe_3O_4.

Note and references

1.X. L. Chen, K. L. Zhong, T. Shi, X. L. Meng, G. L. Wu and Y. Lu, Synthetic Metals, 2019, 248, 59-67.

2.X. M. Feng, R. M. Li, Y. W. Ma, R. F. Chen, N. E. Shi, Q. L. Fan and W. Huang, Adv. Funct. Mater, 2011, 21, 2989-2996.

3.T. Wen, Q. H. Fan, X. L. Tan, Y. T. Chen, C. L. Chen, A. W. Xu and X. K. Wang, Polymer Chemistry, 2016, 7, 785-794.

4.T. Wu, Y. Liu, X. Zeng, T. T. Cui, Y. T. Zhao, Y. N. Li and G. X. Tong, ACS Appl Mater Interfaces, 2016, 8, 7370-7380.

5.J. K. Sun, P. Zan, X. J. Yang, L. Ye and L. J. Zhao, Electrochimica Acta, 2016, 215, 483-491.

6.Y. Liu, Y. W. Fu, L. Liu, W. Li, J. G. Guan and G. X. Tong, ACS Appl Mater Interfaces, 2018, 10, 16511-16520.

7.H. Zeng, J. Li, Z. L. Wang, J. P. Liu and S. H. Sun, Nano Letters, 2004, 4, 187-190.